

Study on the Shock Wave Characteristics of Spherical and Cylindrical Explosives in Near-field Underwater Explosion

J. Yu^{1,2,†}, X. P. Zhang^{1,2}, J. Wang^{1,2,3}, Y. Hao^{1,3} and H. B. Mao^{1,3}

¹ China Ship Scientific Research Center, Wuxi, Jiangsu, 214082, China

² Taihu Laboratory of Deep-sea Technology Science, Wuxi, Jiangsu, 214082, China

³ National Key Laboratory of Ship Structural Safety, Wuxi, China, Wuxi, Jiangsu, 214082, China

†Corresponding Author Email: yujun@cssrc.com.cn

ABSTRACT

Underwater explosions are applied across diverse sectors and present considerable risks to marine infrastructures. Therefore, precise prediction of shockwave loading characteristics for various charge shapes during underwater explosions is critical. This study presents a novel compressible multiphase fluid solver, developed to accurately simulate shockwave propagation and the dynamics of multiphase interfaces. A spatial discretization of the system equations utilizes a fifth-order Weighted Essentially Non-Oscillatory (WENO) scheme for reconstruction, whereas temporal discretization employs a third-order Total Variation Diminishing (TVD) scheme implemented via Runge – Kutta methods. Furthermore, the description of the detonation reaction incorporates a newly developed programmed burn model. The interface dynamics are captured through the application of the level-set method. The solver was initially validated by comparing the propagation results of detonation waves against established data in the literature. Both the simulated peak pressures and shockwave histories closely matched theoretical and experimental data. Different geometries of TNT charges were then analyzed to investigate shockwave propagation in near-field underwater explosions. The newly developed compressible multiphase solver, incorporating detonation reactions, precisely captured the early stages of shockwave propagation. This research offers vital technical insights for accurately predicting shockwave dynamics in near-field underwater explosions in complex scenarios.

Article History

Received July 7, 2024

Revised September 14, 2024

Accepted October 20, 2024

Available online February 4, 2025

Keywords:

Multiphase flows

Shock wave

Underwater explosion

High-order reconstruction

Level-set

1. INTRODUCTION

The impact of charge geometry on shock waves from underwater explosions (UNDEX) represents a vital research domain with considerable relevance to marine engineering, defense initiatives, and environmental science. UNDEX find broad applications ranging from the removal of underwater obstructions and seabed mining to military strategies. It is crucial to comprehend how variations in charge geometries affect shock wave properties to enhance application efficacy and reduce negative impacts on marine ecosystems and structures. The process of UNDEX is categorized into three crucial phases: the initiation of the explosive charge, the transmission of the shock wave, and the oscillation of the resulting bubble (Cole, 1948; Yu. et al., 2021a; Zhang et al., 2023). Each stage is affected by various factors, such as the physical properties of the explosive material, the

characteristics of the surrounding aqueous environment, and the geometric configuration of the charge. The configuration of explosive charges significantly influences the distribution of shock wave intensity, peak pressures, and impulses in both spatial and temporal dimensions. Studies of underwater detonations trace back to the late 19th century but saw substantial progress during the world conflicts of the 20th century. This period marked the development of sophisticated analytical techniques and a deeper comprehension of the associated physical dynamics.

Numerous scholars have made significant contributions to research on underwater explosion shockwaves. Hilliar (1950) conducted a qualitative analysis of shockwave propagation characteristics based on systematic underwater explosion experiments. Through similarity analysis, Hilliar first proposed the basic form of the underwater explosion similarity law.

[Kennard \(1950\)](#) addressed various aspects of explosion shockwaves, including propagation, secondary pressure waves, similarity laws, and lagging flows, using qualitative theoretical analysis. To explore the propagation laws and spatiotemporal distribution characteristics of underwater explosion shockwaves, [Penney and Dasgupta \(1950\)](#) applied compressible flow equations along characteristic lines. [Blaik and Christian \(1964\)](#) significantly enhanced existing semi-empirical formulas for parameters such as shockwave rise time, peak pressure, and decay time. [Baum and Sanasaryan \(1965\)](#) conducted a study on how hydrostatic pressure affects the shockwave load from UNDEX. His findings demonstrated that the impulse of the shockwave changes proportionally to the power of 1/6.

In UNDEX, interactions between multiple phases—namely unreacted explosives, their gaseous byproducts, and the ambient water—are crucial. Accurate simulations require detailed representation of these phases and precise modeling of shockwave dynamics. Two predominant approaches for modeling the detonation process are the Detonation Shock Dynamics model (DSD) and the Instantaneous Detonation Model (IDM) ([Yu et al., 2024a](#)). The DSD approach integrates a theoretical model to track detonation wave fronts with subsequent numerical calculations of the flow of gaseous products post-detonation ([Bdzil et al., 2001](#); [Handley et al., 2018](#)). The IDM simplifies the initial conditions by omitting stages like ignition and detonation propagation, instead using mass or energy equivalences to estimate the state of gaseous products immediately after detonation. For capturing the interfaces between phases, the Volume Of Fluid (VOF) method is widely employed, with each computational cell containing a mixture of fluids represented by a function that delineates the volume fractions of each component ([Benson, 1992](#); [Miller & Puckett, 1996](#)). Another method based on the level-set approach captures the interface location ([Mulder et al., 1992](#); [Osher & Fedkiw, 2001](#)).

It is known that the shape of the charge significantly influences airblast characteristics, particularly in the near-field. Research focusing on the pressure-distance relationships for various shaped charges such as spherical, cylindrical, and rectangular forms has been carried out through both experimental and numerical methods ([Knock & Davies, 2013](#)). Despite extensive analyses on cylindrical charges generating air blasts ([Plooster, 1982](#)), the data on other non-spherical shapes remain sparse. It has been consistently observed across various studies that the highest pressures and impulses are directed towards the side with the greatest surface area of the explosive. For instance, cylindrical explosives with a smaller length-to-diameter (L/D) ratio emit the majority of their blast energy axially, whereas those with a higher L/D ratio disperse more energy radially. [Yu et al. \(2024b\)](#) utilized a multiphase flow compressible fluid solver that accounted for detonation effects to analyze and compare the initial shock wave impacts from strip explosives detonating in water and air.

Despite these advancements, the specific impact of charge shapes on shock wave characteristics still requires

further investigation. Different geometries, such as spherical, cylindrical, and conical, produce distinct shock wave profiles. These variations significantly affect the performance of underwater explosion applications and the loading on adjacent structures. This study explores the effects of various charge shapes on the propagation of shock waves in UNDEX. By utilizing advanced computational fluid dynamics (CFD) simulations and corroborating the results with experimental data, this research aims to comprehensively understand the influence of charge geometry on shock wave dynamics. The outcomes of this research will enhance the accuracy of predictive modeling and refine design protocols for underwater detonations utilized across various engineering fields and military operations.

Research on the impact of the geometry of charges on shockwaves produced by near-field UNDEX remains largely unexplored, with significant aspects still to be discovered. In this study, a numerical simulation model of a compressible multiphase solver with a detonation reaction is presented. Several numerical examples validate and apply this method in cases involving the propagation of detonation and shock waves. Subsequently, simulations of two different TNT charge shapes are conducted to compare shock wave propagation in near-field UNDEX. Finally, the research findings are concisely summarized in the conclusions.

2. NUMERICAL SIMULATION METHOD

The compressible and inviscid Euler fluid in the two-dimensional space is used as an example to introduce the fluid dynamics. The behavior of the fluid adheres to the equation delineated below ([Yu et al., 2021a, 2024b](#))

$$\frac{\partial \mathbf{U}}{\partial t} + \frac{\partial \mathbf{F}(\mathbf{U})}{\partial x} + \frac{\partial \mathbf{G}(\mathbf{U})}{\partial y} = \mathbf{S}(\mathbf{U}) \quad (1)$$

$$\mathbf{U} = \begin{pmatrix} \rho \\ \rho u \\ \rho v \\ \rho E \end{pmatrix}, \quad \mathbf{F}(\mathbf{U}) = \begin{pmatrix} \rho u \\ \rho u^2 + p \\ \rho uv \\ (\rho E + p)u \end{pmatrix}, \quad (2)$$

$$\mathbf{G}(\mathbf{U}) = \begin{pmatrix} \rho v \\ \rho uv \\ \rho v^2 + p \\ (\rho E + p)v \end{pmatrix}, \quad \mathbf{S}(\mathbf{U}) = -\frac{n}{x} \begin{pmatrix} \rho u \\ \rho u^2 \\ \rho uv \\ (\rho E + p)u \end{pmatrix}$$

In this fluid dynamics model, ρ , p and E signify the density, pressure and specific total energy of the fluid, respectively. The components u and v represent the velocities along the x and y coordinates. The formula for specific total energy is expressed as $E = e + 0.5(u^2 + v^2)$, where e indicates the specific internal energy. The parameter n determines the dimensional context of the flow, assuming values of 0, 1, or 2. Specifically, a 2D plane flow corresponds to $n = 0$, a 2D axisymmetric flow to $n = 1$, a 1D plane flow to $n = 0$ with $v = 0$, a 1D cylindrical flow to $n = 1$ with $v = 0$, and a 1D spherical flow is denoted by $n = 2$ with $v = 0$.

Table 1 Properties for high explosive materials.

	$A(\text{GPa})$	$B(\text{GPa})$	R_1	R_2	ω
TNT	371.2	3.21	4.15	0.95	0.3
RS211	758.0	8.51	4.9	1.1	0.2

In System (1), the dynamics of water and gaseous products are effectively modeled using the stiffened gas (SG) and Jones-Wilkins-Lee (JWL) equations. The latter is favored for numerical simulations across various proprietary and open-source platforms, due to its straightforwardness and computational efficiency. The JWL EOS incorporates multiple parameters that define the interrelations of pressure, relative volume, and internal energy within detonation products. These parameters are ascertainable through the expansion tests conducted on metal cylinders (Price et al., 2015). The JWL EOS can be described as

$$p = A \left(1 - \frac{\omega}{R_1 \bar{V}} \right) e^{-R_1 \bar{V}} + B \left(1 - \frac{\omega}{R_2 \bar{V}} \right) e^{-R_2 \bar{V}} + \omega \rho e \quad (3)$$

where e and \bar{V} , represent the internal energy and the relative volume ($\bar{V} = \rho_0 / \rho$), respectively. The initial density of the explosive is denoted by ρ_0 , while A , B , R_1 , R_2 , and ω are parameters specific to a given explosive type. Table 1 displays the JWL EOS characteristics for both TNT and RS211 explosives (Price et al., 2015; Sheng et al., 2023).

In the modeling of water and air as fluids, the SG equation of state is commonly employed. (Yu et al., 2021a, 2022)

$$p = \rho e (\gamma - 1) - \gamma P_\infty \quad (4)$$

where the constants γ and p_∞ define properties intrinsic to the material, while p_∞ represents a pressure-related parameter derived from empirical adjustments aligned with experimental findings. It is advised that values $\gamma = 7.42$, $p_\infty = 296 \text{MPa}$ be utilized specifically for water (Yu et al., 2024b).

The programmed burn model is designed to simulate the transformation of unreacted energetic substances into gaseous products and the liberation of energy from chemical detonations. This model necessitates determining the burn factor, denoted as λ , for each explosive cell (Yu et al., 2024b)

$$\lambda_1 = \frac{(t - t_c) D_{CJ} + w_z / 2}{w_z} \quad (5)$$

$$\lambda_2 = H(\bar{V}) \frac{1 - \bar{V}}{1 - \bar{V}_{CJ}}, \quad H(\bar{V}) = \begin{cases} 1, & \text{for } \bar{V} \geq \bar{V}_{CJ} \\ 0, & \text{otherwise} \end{cases} \quad (6)$$

$$\lambda = \min(\max(0, \lambda_1, \lambda_2), 1) \quad (7)$$

The moment, t_c , at which the detonation wave impacts the center of a cell laden with explosives is defined by the cell equivalent size, w_z , and the detonation velocity, D_{CJ} . The density at the CJ state is denoted as

\bar{V}_{CJ} , which corresponds to a relative density where $\bar{V}_{CJ} = \gamma / (\gamma + 1)$, and $\gamma = \sqrt{1 + D_{CJ} \rho_0 / 2 / Q_0}$.

In the dynamic simulation of multiphase fluid flows, the level-set model is employed to track the evolving interfaces between the phases (Osher & Fedkiw, 2001). At the commencement of each simulation step, a signed distance function, denoted as $\phi(r, z)$, is utilized to characterize the initial spatial arrangement of the fluids within the two phases. The location of each phase is updated by

$$\phi_t + u \phi_r + v \phi_z = 0 \quad (8)$$

In order to capture the shock waves impacting on the multiphase interface, the MGFM is adopted to provide expanded stencils for the grids on the multiphase interface. A two-shock approximation solver is performed at the interface. The details of MGFM for SG EOS had been provided by Liu et al. (2003). To effectively model the dynamics of detonation and shock waves, particularly when dealing with high-pressure and high-density environments, advanced computational techniques are essential. The WENO scheme, developed by Shu and Osher (1988), is frequently employed in the simulation of compressible fluids. This scheme excels at managing the challenges posed by shock waves and intricate smooth flow structures. It begins with the local decomposition of numerical fluxes into their characteristic fields. Following this, a high-order reconstruction ensures that the fluxes are accurately reconstituted in physical space (Wang et al., 2017). For the integration of the Euler equations over time, a third-order TVD Runge-Kutta method is implemented (Shu & Osher, 1988).

3. VALIDATION OF THE METHOD

In this section, we perform a series of numerical and theoretical tests on shock waves in explosives and water to validate our numerical method. Initially, a one-dimensional (1D) test compares the detonation wave propagation from our model with established results in the literature. Subsequent simulations of UNDEX employ a 1D spherical symmetry model for comparison with theoretical predictions.

3.1 1D Detonation Wave Validation

In underwater detonation scenarios, initiating an explosive generates detonation shock waves within the charge, which then propagate outward, eventually impacting the surrounding water after exiting the surface of the charge. A common benchmark for evaluating numerical detonation simulations involves the use of a 1D TNT slab, ignited at one extremity. This discussion will focus on a TNT slab, 0.1m in length, analyzed in a simulation by Liu using the Smoothed Particle Hydrodynamics (SPH) method, which effectively demonstrated the wave travel through the explosive material (Liu & Liu, 2010). To mimic a centrally ignited 0.2 m long slab, a symmetric condition was implemented at the ignition point. Specifications of the TNT are presented in Table 1. The analysis domain extends from 0

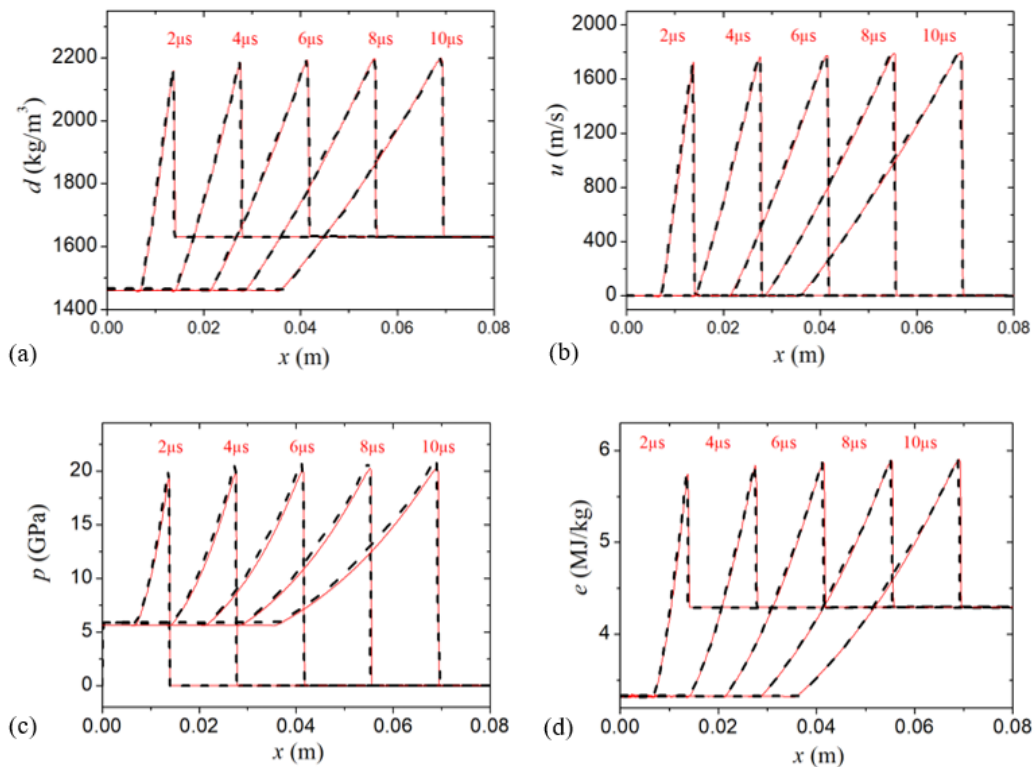


Fig. 1 Comparative Analysis of TNT Charge Characteristics at Various Time Intervals: Numerical density profiles are shown in (a), velocity in (b), pressure in (c), and internal energy in (d) at time increments of $t = 2, 4, 6, 8$ and $10 \mu s$. Solid red lines represent the current solution, while dashed black lines indicate the solution as reported by Liu

reflect Liu data, showing a strong correlation between the methodologies.

The subsequent analysis evaluates the grid convergence in the programmed burn model. Displayed in Fig. 2 are the comparisons among profiles of density, velocity, pressure, and internal energy at $t = 8 \mu s$, utilizing mesh dimensions that vary from 1 mm down to 0.001 mm as illustrated in Fig. 2, increasing the grid density leads to a higher peak value at the wave front. The numerical results show that the solutions with $dx = 0.1$ mm meet the precision requirements for engineering applications, while the solutions with $dx = 0.01$ mm are very close to the convergence values. The results with $dx = 0.001$ mm can be used as a reference for exact solutions. The simulations demonstrate convergence of the programmed burn model and confirm the accuracy of the detonation wave speeds derived for the 1D spatial analysis.

3.2 Shock Wave Validation in Water

In the vicinity of an underwater explosion, the near-field includes areas immediately adjacent to or within the gas products released by the detonation. This zone is defined by intense shock waves and intricate patterns of shock profiles due to the dynamic exchanges between the gaseous byproducts of the detonation and the adjacent aquatic environment. The theoretical model of shock wave pressure in water has been well summarized by Cole (1948). In this section, a series of UNDEX cases are simulated using a 1D spherical symmetry model with TNT

charges of varying masses: 0.1 kg, 1 kg, and 10 kg. All simulations are conducted with a mesh size of $\delta = 0.1$ mm. Fig. 3 compares the simulated shock wave pressure histories to theoretical solutions at four typical points with different distance-to-radius ratios of $r/R_0 = 10, 20, 40,$ and 60 , while R_0 is the radius of explosive charge. Across various charge masses, the numerical findings consistently align well with theoretical predictions.

4. RESULTS AND DISCUSSIONS

The established numerical technique for analyzing compressible multiphase flows is applied here to explore the characteristics of shock wave loads arising from the detonation of spherical and cylindrical explosive charges. First, the physical problem is delineated, specifying the initial conditions for the simulation which include the computational domain and the configurations of the charges. Two distinct charge shapes are described, with several r/R_0 ratios established for subsequent analysis. Next, the numerical outcomes for both spherical and cylindrical charges are detailed. The manuscript concludes with a comparison of the shock wave properties between the different charge shapes, drawing conclusions from these observations.

4.1 Physical Problem Describing

It is well known that the shape of an explosive charge significantly influences the near-field underwater explosion dynamics. Experimental investigations were

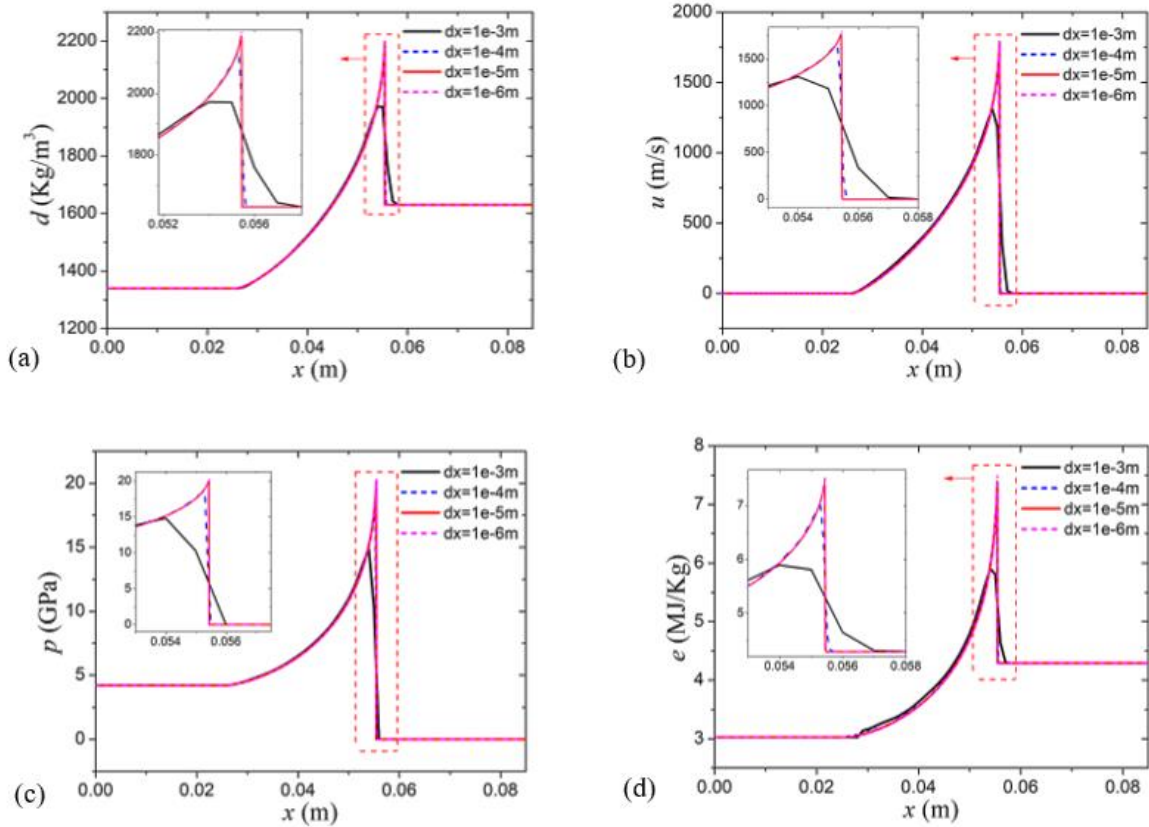


Fig. 2 Detailed Examination of TNT Charge Properties at 8 μ s Post-Detonation: Displays profiles for numerical density (a), velocity (b), pressure (c), and internal energy (d)

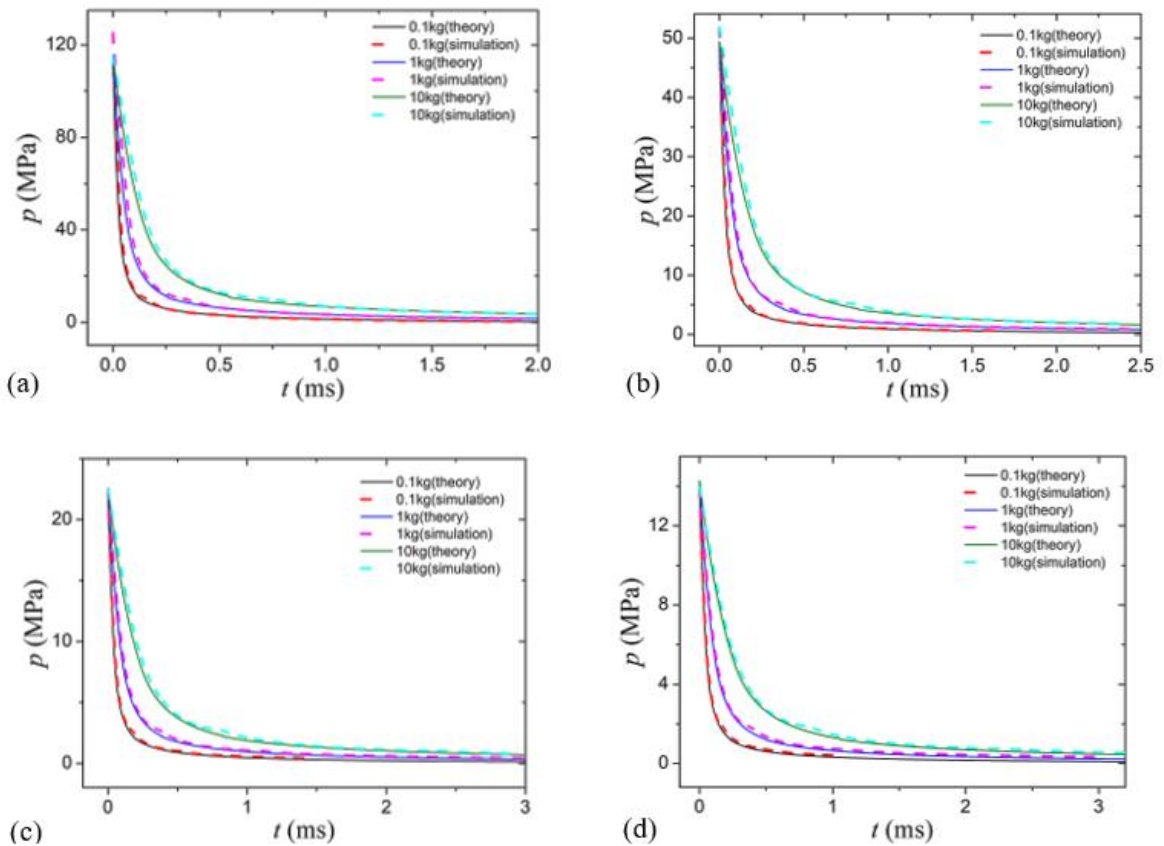


Fig. 3 Numerical results of pressure profiles are compared with theoretical solutions at four typical points. (a) $r/R_0= 10$; (b) $r/R_0= 20$; (c) $r/R_0= 40$; (d) $r/R_0= 60$

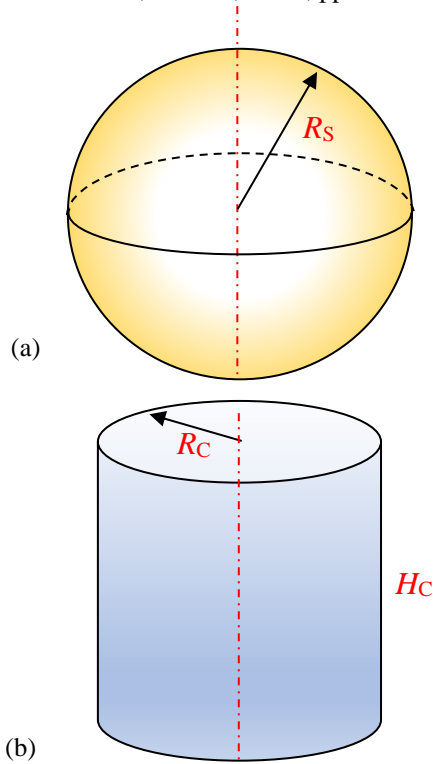


Fig. 4 Schematic diagram of spherical (a) and cylindrical (b) shape charges. The radius of spherical charge is R_s . The radius and height of the cylindrical charge are R_c and H_c . The initiation point is located at the center of the sphere and cylinder, respectively

conducted to establish the correlations between pressure and distance for charges of spherical, cylindrical, and rectangular geometries. Extensive research on UNDEX using spherical charges has been conducted through both experimental and numerical approaches. However, data on non-spherical geometries remain scarce. The primary challenges in studying near-field UNDEX stem from capturing the interaction between multiphase flow interfaces and detonation reactions, as well as accurately tracking shock wave propagation. As a result, the intricate behavior of near-field UNDEX with non-spherical charges in deep water remains inadequately understood.

In this section, near-field UNDEX using spherical and cylindrical TNT charges with a 2D axisymmetric model are examined (Fig. 4). The computational domain measures $[-1.2, 1.2] \times [-1.2, 1.2] \text{ m}^2$, with a mesh size of $\delta = 0.5 \text{ mm}$. Charge centers are located at the origin of the coordinate system. Both the diameter (R_c) and height (H_c) of the cylindrical charge are 42 mm. To facilitate comparison, the volume and density of the spherical charge are equal to those of the cylindrical charge, resulting in a spherical charge radius of approximately 24 mm. These charges are initiated at the center of their respective volumes. Various r/R_0 ratio points are established to record the pressure histories in axial and radial directions (Fig. 5). Points A1, A2, A3, and A4 represent the axial direction, while points B1, B2, B3, and B4 represent the radial direction. The boundary is set to a non-reflection condition.

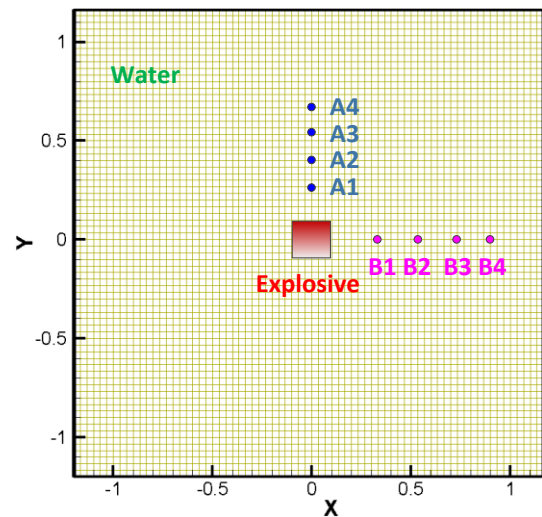


Fig. 5 Schematic diagram of the computational domain. The mesh density shown in the figure is 1/50 of the actual mesh density

4.2 Explosion of the Spherical Charge

Phenomena associated with UNDEX are subject to a range of physical principles and conditions, particularly at the interface where explosive material and water meet. It is crucial to define a physical linkage between the detonation process and the resultant wave disturbances. In the vicinity of an underwater explosion, water exhibits dynamic behavior, characterized by elevated pressures which influence the speed of wave propagation. Following the detonation, secondary pressure waves emerge, with shock waves becoming predominant over certain ranges. As the detonation front contacts the external boundary of the cylindrical explosive cross-section, a complex interplay unfolds between unreacted explosive material, gaseous byproducts, and surrounding water. This interaction leads to strong shock wave propagation in the surrounding water, with some explosive continuing to detonate.

Numerical results for density, pressure, and interface profiles during the early detonation stage are shown in Fig. 6. At $t = 1 \mu\text{s}$, the detonation wave has just been generated and is propagating through the explosive. A significant amount of unreacted charge surrounds the detonation wave, with the maximum pressure reaching approximately 15 GPa. At $t = 3 \mu\text{s}$, the detonation waves have reached the surface of the spherical charge, completing the chemical reaction. At $t = 5 \mu\text{s}$, a pronounced shockwave is produced in the aquatic environment, concurrently with the onset of rarefaction waves moving towards the static zone of internal gas products. At $t = 10 \mu\text{s}$, the gaseous bubble exhibits regions of low density and pressure, except for a minor central area where pressure remains high. Numerical analyses delineate density, pressure, and boundary evolution during this phase of shockwave movement in water, as illustrated in Fig. 7. The propagation of the shockwave through water prompts the bubble to expand outward. Following the detonation of the spherical charge in an unconfined setting, the shockwave retains its spherical configuration as it travels through the water.

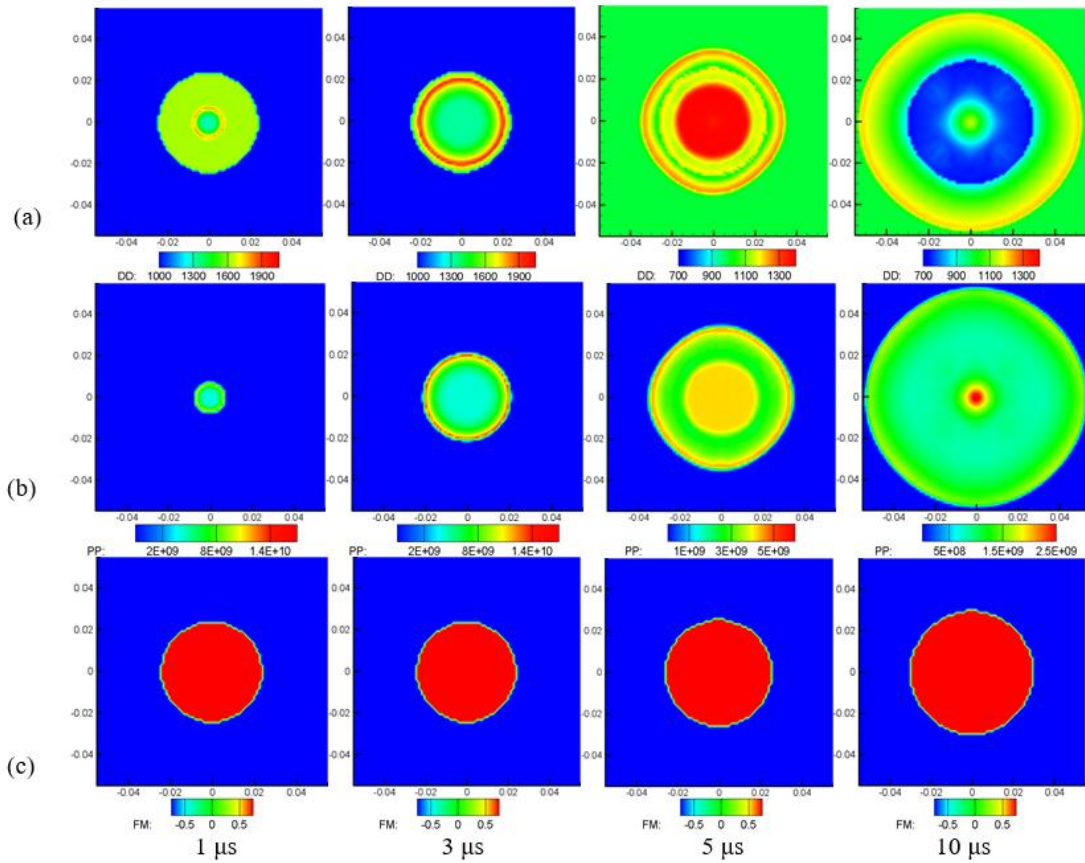


Fig. 6 Numerical results of density (a), pressure (b), and interface (c) contours for a spherical TNT charge during early detonation stage at $t = 1, 3, 5, 10\mu\text{s}$

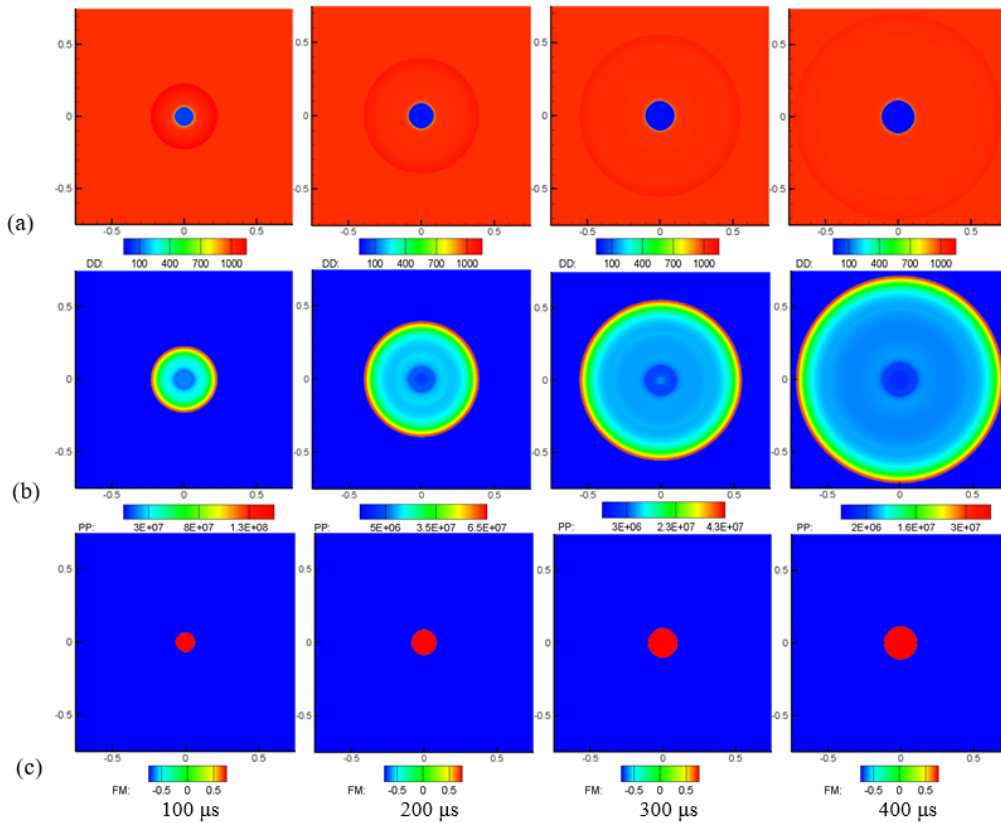


Fig. 7 Numerical results of density (a), pressure (b), and interface function (c) contours for a spherical TNT charge during shockwave in water stage at $t = 100, 200, 300, 400\mu\text{s}$

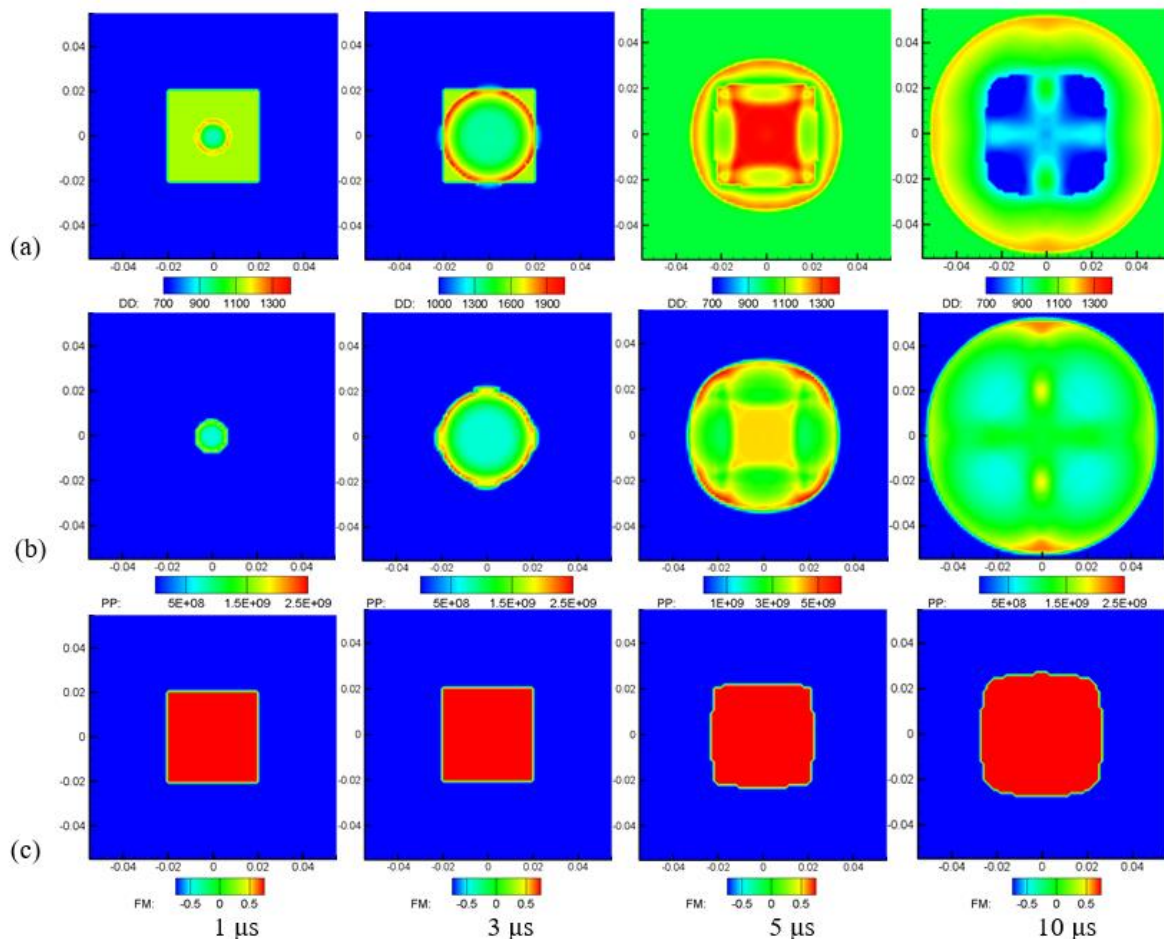


Fig. 8 Numerical results of density (a), pressure (b), and interface (c) contours for a cylindrical TNT charge during early detonation stage at $t = 1, 3, 5, 10\mu\text{s}$

4.3 Explosion of the Cylindrical Explosive Charge

When the cylindrical TNT charge is centrally initiated (Fig. 4), interactions occur among the unreacted explosive, gaseous products, and water. The detonation wave propagates downward in a fan-shaped manner within the charge. Numerical results illustrate changes in density, pressure, and interface profiles during the early stages of detonation (Fig. 8). By $t = 1 \mu\text{s}$, initiation of the detonation wave occurs, with its subsequent propagation through the explosive material. At $t = 3 \mu\text{s}$, the leading edge of this wave encounters the outer boundary of the explosive, positioning a minimal quantity of yet-to-react material in its forefront. At $t = 5 \mu\text{s}$, this reaction sequence culminates, resulting in the generation of a potent shock wave that permeates the surrounding water. Simultaneously, a rarefaction wave begins to propagate inward from all sides of the bubble. At $t = 10 \mu\text{s}$, low-density and low-pressure regions are observed within the gaseous bubble, with only a small high-pressure area remaining in the explosive.

Numerical results for density, pressure, and interface profiles during the shockwave propagation stage in water are shown in Fig. 9. The propagation of the shock wave in aquatic environments persists radially, as the expansion of the gaseous bubble ensues. The density and pressure distributions within the bubble are highly nonlinear. Between $100 \mu\text{s}$ and $400 \mu\text{s}$, as shown in Fig. 9, the

shockwave front gradually assumes a spherical shape as it propagates through the water.

4.4 Comparison Analysis and Discussion

The pressure history profiles at different r/R_0 ratio points for spherical and cylindrical TNT charges are compared in Fig. 10. Comparative analysis reveals that the pressure profiles along the axial direction in cylindrical and spherical charges exhibit similarities, although a minor variation is evident at $r/R_0 = 5$. However, the pressure history in the radial direction for the cylindrical TNT differs from the other two points. This trend is observed at the other three r/R_0 ratio points as well.

Figure 11 presents a comparative analysis of the time-history curves for both the equivalent radius and the expansion velocity of the explosion bubble, contrasting these metrics between the two different charge configurations. Because the aspect ratio of the cylindrical charge is close to 1, the bubble radius and expansion velocity produced by the two charges are almost identical. Meanwhile, Fig. 12 presents the temporal progression curves for the equivalent radii and velocities of shockwave positions associated with two different charge configurations. Initially, the differences between these configurations are minimal upon the completion of detonation. Figure 13 illustrates the temporal progression curves depicting both the total internal energy and the total kinetic energy within the explosion bubbles. At the onset of

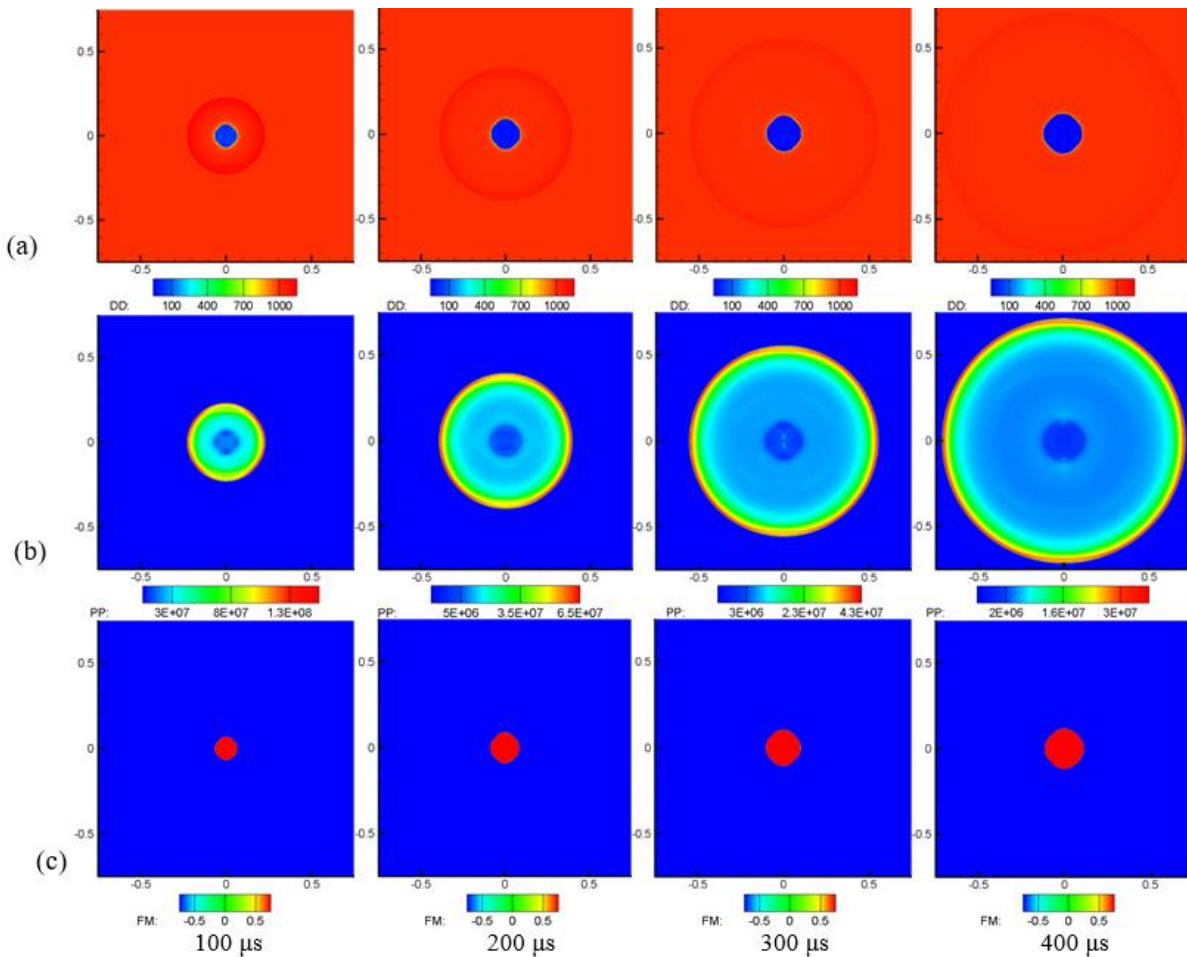


Fig. 9 Numerical results of density (a), pressure (b), and interface (c) contours for a cylindrical TNT charge during shockwave in water stage at $t = 100, 200, 300, 400 \mu s$

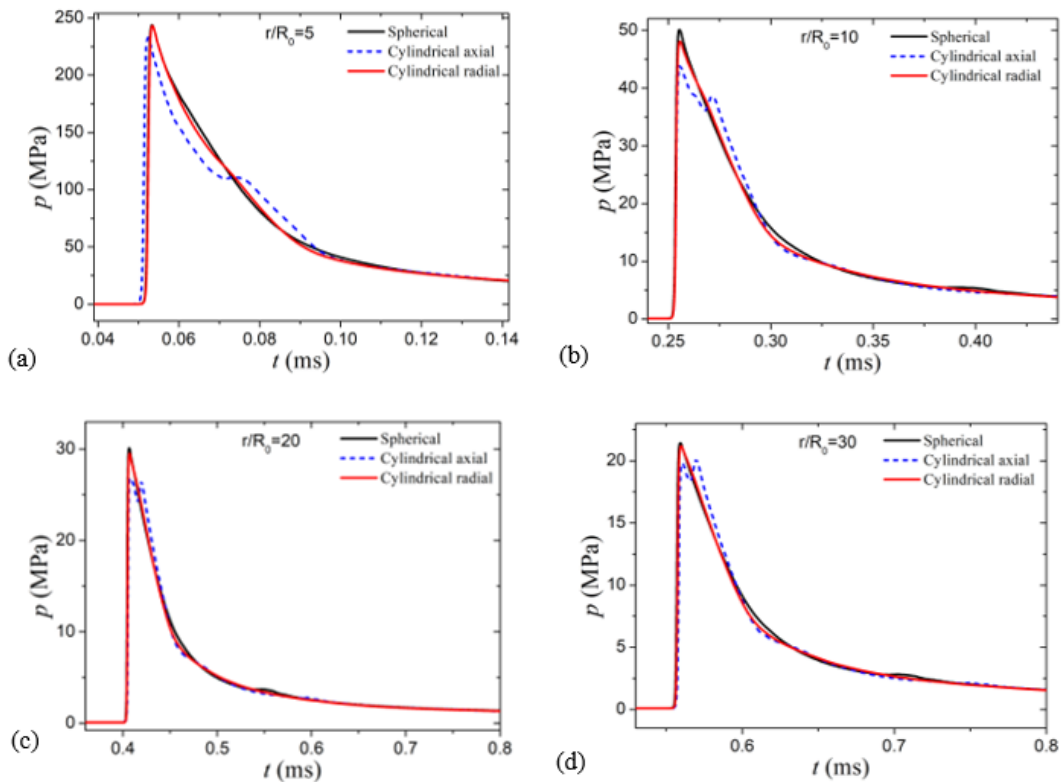


Fig. 10 Pressure histories at different distance-to-radius (r/R_0) points under the spherical and cylindrical TNT charges. (a) $r/R_0 = 5$; (b) $r/R_0 = 10$; (c) $r/R_0 = 20$; (d) $r/R_0 = 30$

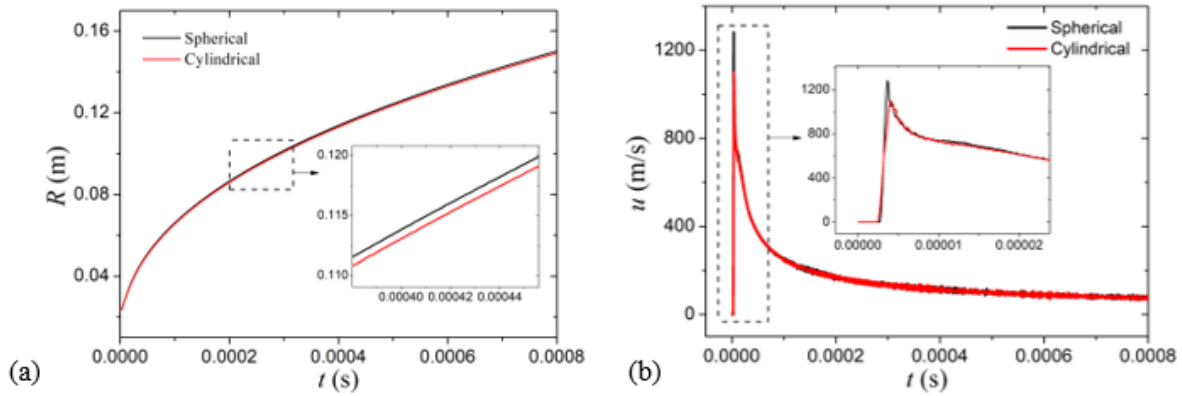


Fig. 11 Comparison of time-history curves of equivalent radius (a) and expansion velocity (b) for the explosion bubble

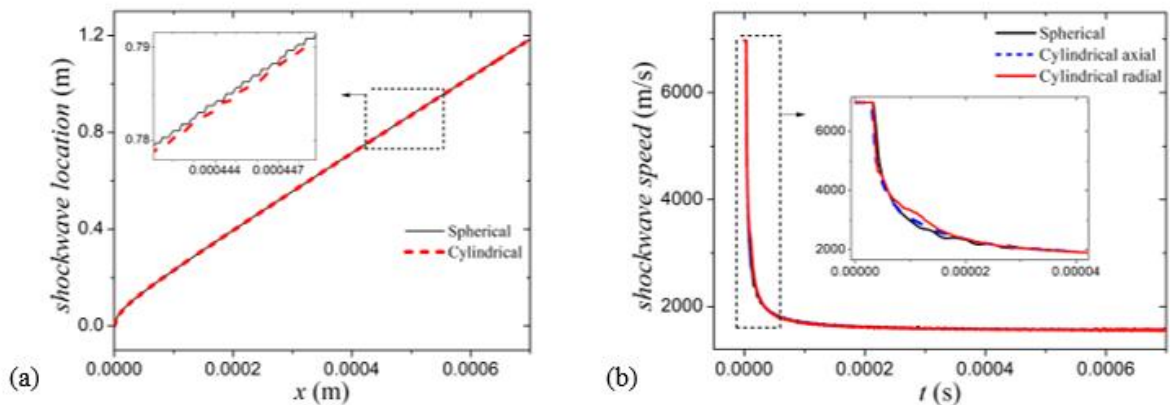


Fig. 12 Time history curve of the equivalent radius of shockwave location (a) and equivalent speed (b) for two charge shapes

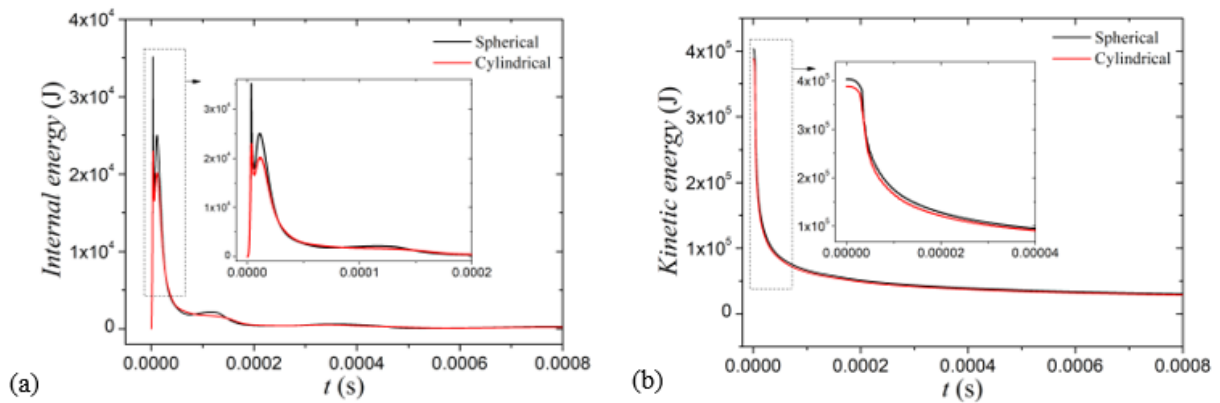


Fig. 13 Time history curve of total internal energy (a) and total kinetic energy (b) of the explosion bubbles

the detonation phase, the internal energy of the bubble produced by a spherical TNT charge exceeds that from a cylindrical charge, suggesting that the spherical configuration is more efficient for the explosive's energy release.

5. CONCLUSION

In this study, we analyze the characteristics of detonation waves and shock loads for spherical and cylindrical shaped charges, employing a compressible

multiphase fluid solver developed with high-order finite difference schemes. Discretization of the spatial components in the system equations employs fifth-order WENO reconstruction within characteristic spaces, complemented by Lax-Friedrich splitting technique. Concurrently, the temporal components are treated via a third-order TVD Runge–Kutta method. The process of generating and propagating detonation waves is modeled through a programmed burn approach, whereas the level-set technique, integrated with the MGFM scheme, effectively tracks the multiphase interfaces. A series of

both numerical and experimental tests involving shock waves in explosives and water was conducted to validate the numerical method. In the context of the 1D detonation wave propagation issue, the existing model aligns well with the SPH model. The computational outcomes indicate convergence of the programmed burn model currently in use, ensuring accurate velocities of detonation waves in 1D space.

The geometry of the explosive charge plays a crucial role in influencing the behavior of UNDEX, particularly within the near-field region. To analyze the shockwave loading characteristics associated with spherical and cylindrical charges, a solver designed for compressible multiphase flows is employed. Initially, the physical problem, including the initial conditions of the simulation such as the computational domain and the configuration of the charge, is described. Two charge shapes are introduced in this section, along with varied r/R_0 ratios. Subsequently, the numerical results for both spherical and cylindrical charges are detailed. Finally, the manuscript presents a comparison of the different shapes and provides some conclusions. According to numerical simulations, when the detonation wave front arrives at the external boundary of the cross-sectional area of the cylindrical charge, intricate interactions occur involving the unreacted explosive material, gaseous detonation products, and surrounding water.

CONFLICT OF INTEREST

The authors declare that there are no conflicts of interest to disclose.

DATA AVAILABILITY

The data that support the finding of this study are available from the corresponding author upon reasonable request.

AUTHORS CONTRIBUTION

J. Yu: Conceptualization, Methodology, Software, Validation, Formal analysis, Investigation, Writing – Review & Editing. **X. Zhang:** Conceptualization, Resources, Data Curation, Visualization. **J. Wang:** Methodology, Software, Validation, Formal analysis, Investigation, Data Curation. **Y. Hao:** Resources, Formal analysis. **H. B. Mao:** Conceptualization, Visualization.

REFERENCES

- Baum, F. A., & Sanasaryan, N. S. (1965). Effect of hydrostatic pressure on the parameters of an underwater explosion. *Combustion, Explosion, and Shock Waves*, 1 (4), 52-62. <http://doi.org/10.1007/BF00743521>
- Bdzil, J. B., Stewart, D. S., & Jackson, T. L. (2001). Program burn algorithms based on detonation shock dynamics: Discrete approximations of detonation flows with discontinuous front models. *Journal of Computational Physics*, 174, 870-902. <http://doi.org/10.1006/jcph.2001.6934>
- Benson, D. J. (1992). Computational methods in Lagrangian and Eulerian hydrocodes. *Computer Methods in Applied Mechanics and Engineering*, 99, 235-394. [http://doi.org/10.1016/0045-7825\(92\)90042-1](http://doi.org/10.1016/0045-7825(92)90042-1)
- Blaik, M., & Christian, E. A. (1964). Pressure pulses of small explosions at great depths in the ocean. 68th Meeting, Acoust. Soc. Am, Austin, Texas (1964). <https://doi.org/10.1121/1.1939301>
- Cole, R. H. (1948). *Underwater explosion*. Princeton University Press, New Jersey.
- Handley, C. A., Lambourn, B. D., Whitworth, N. J., James, H. R., & Belfield, W. J. (2018). Understanding the shock and detonation response of high explosives at the continuum and meso scales. *Applied Physics Reviews*, 5, 011303. <http://doi.org/10.1063/1.5018290>
- Hilliard, H. W. (1950). *Experiments on the pressure wave thrown out by submarine explosions*. Department of the Navy, Office of Naval Research, Washington, D.C., 86-158.
- Kennard, E. H. (1950). *Report on underwater explosions*. Department of the Navy, Office of Naval Research, Washington, D.C., 159-208.
- Knock, C., & Davies, N. (2013). Blast waves from cylindrical charges. *Shock Waves*, 23, 337-343. <http://doi.org/10.1007/s00193-013-0441-1>
- Liu, G. R., & Liu, M. B. (2010). *Smoothed particle hydrodynamics: A meshfree particle method*. World Scientific Publishing, Singapore, <http://doi.org/10.1142/9789812779240>
- Liu, T., Khoo, B., & Yeo, K. (2003). Ghost fluid method for strong shock impacting on material interface. *Journal of Computational Physics*, 190, 651-681. [http://doi.org/10.1016/S0021-9991\(03\)00203-8](http://doi.org/10.1016/S0021-9991(03)00203-8)
- Miller, G. H., & Puckett, E. G. (1996). A high-order Godunov method for multiple condensed phases. *Journal of Computational Physics*, 128(1), 134-164. <http://doi.org/10.1006/jcph.1996.0200>
- Mulder, W., Osher, S., & Sethian, J. A. (1992). Computing interface motion in compressible gas dynamics. *Journal of Computational Physics*, 100, 209-228. [http://doi.org/10.1016/0021-9991\(92\)90227-C](http://doi.org/10.1016/0021-9991(92)90227-C)
- Osher, S., & Fedkiw, R. (2001). Level set methods: An overview and some recent results. *Journal of Computational Physics*, 169, 463-502. <http://doi.org/10.1006/jcph.2000.6636>
- Penney, W. G., & Dasgupta, H. K. (1950). *The pressure-time curve for underwater explosions (II)*. Department of the Navy, Office of Naval Research, Washington, D.C., 289-300.
- Plooster, M. N. (1982). *Blast effects from cylindrical explosive charges: Experimental measurements*. Naval Report Centre, China Lake, California 93555.

- Price, M. A., Nguyen, V. T., Hassan, O., & Morgan, K. (2015). A method for compressible multimaterial flows with condensed phase explosive detonation and airblast on unstructured grids. *Computers & Fluids*, 111, 76-90. <http://doi.org/10.1016/j.compfluid.2014.05.001>
- Sheng Z., Hao Y., Liu J., Wang H., Gao Y. & Ma, F. (2023). A shockwave calculation method for aluminized explosive of deep water explosion based on the Kirkwood-Bethe model. *Propellants, Explosives, Pyrotechnics*, 48, e202200247. <https://doi.org/10.1002/prep.202200247>
- Shu, C. W., & Osher, S. (1988). Efficient implementation of essentially non-oscillatory shock-capturing schemes, *Journal of Computational Physics*, 77, 439-471. [http://doi.org/10.1016/0021-9991\(88\)90177-5](http://doi.org/10.1016/0021-9991(88)90177-5)
- Wang, L., Currao, G. M. D., Han, F., Neely, A. J., Young, J., & Tian, F. B. (2017). An immersed boundary method for fluid–structure interaction with compressible multiphase flows. *Journal of Computational Physics*, 346, 131-151. <http://doi.org/10.1016/j.jcp.2017.06.048>
- Yu, J., Liu, G. Z., Wang, J., & Wang, H. K. (2021a). An effective method for modeling the load of bubble jet in underwater explosion near the wall. *Ocean Engineering*, 220, 108408. <http://doi.org/10.1016/j.oceaneng.2020.108408>
- Yu, J., Liu, J. H., Wang, H. K., Wang, J., Zhang, L. P., & Liu, G. Z. (2021b). Numerical simulation of underwater explosion cavitation characteristics based on phase transition model in compressible multicomponent fluids. *Ocean Engineering*, 240, 109934. <http://doi.org/10.1016/j.oceaneng.2021.109934>
- Yu, J., Liu, J. H., Wang, H. K., Wang, J., Zhou, Z. T., & Mao, H. B. (2022). Application of two-phase transition model in underwater explosion cavitation based on compressible multiphase flows. *AIP Advances*, 12, 025209. <http://doi.org/10.1063/5.0082209>
- Yu, J., Wang, J., Zhang, X. P., Hao, Y., Jiang, X. W., & Shen, C. (2024a). A high precision instantaneous detonation model (hp-IDM) for condensed energetic materials and its application in underwater explosions. *Journal of Applied Physics*, 136, 044701. <https://doi.org/10.1063/5.0220493>
- Yu, J., Zhang, X. P., Chen, J. P., & Xu, Y. Q. (2024b). A high-order simulation method for compressible multiphase flows with condensed-phase explosive detonation in underwater explosions. *Physics of Fluids*, 36, 016133. <http://doi.org/10.1063/5.0134567>
- Zhang, A. M., Li, S. M., Cui, P., Li, S., & Liu, Y. L. (2023). A unified theory for bubble dynamics. *Physics of Fluids*, 35, 033323. <http://doi.org/10.1063/5.0123456>